International Conference on Space Optics—ICSO 2024

Antibes Juan-les-Pins, France 21-25 October 2024

Edited by Philippe Kubik, Frédéric Bernard, Kyriaki Minoglou and Nikos Karafolas

Straylight assessment for the Venus Emissivity Mapper instrument: requirement definition, design mitigations, and analysis





Straylight assessment for the Venus Emissivity Mapper instrument: requirement definition, design mitigations, and analysis

Martin Pertenais^a, Eitan Pechevis^b, Jean-Michel Reess^b, Julie Bonnetto^c, Ingo Walter^a, Thomas Säuberlich^a, Till Hagelschuer^a, Tristan Buey^b, Gisbert Peter^a, Giulia Alemano^d, and Jörn Helbert^d

^aInstitute of Optical Sensor Systems, German Aerospace Center (DLR), Rutherfordstr. 2, 12489 Berlin, Germany

bLESIA, Observatoire de Paris, 5 place Jules Janssen, 92190 Meudon, France
cPISEO, Parc Lyon Sud, 4 rue de l'Arsenal, 69200 Venissieux, France
dInstitute of Planetary Research, German Aerospace Center (DLR), Rutherfordstr. 2, 12489
Berlin, Germany

ABSTRACT

The Venus Emissivity Mapper (VEM) instrument (on EnVision called VenSpec-M), is a multispectral imager for mapping of the Venus surface and its lower atmosphere, developed at DLR Berlin. This is realized by observation through narrow-band atmospheric windows present in the near-infrared spectral region. VEM will allow to detect thermal emissions like volcanic activity, surface rock composition, water abundance and cloud formation over Venus' surface. The optical design of the instrument includes a single lens imaging Venus's surface on a filter assembly composed by 14 individual filter's tripes, and a 2-lenses relay optic re-imaging this spectrally filtered image onto an InGaAs detector. Considering the low intensity level of the scientific signal the instrument is aiming to detect, any external contributor to the effective Signal to Noise Ratio has to be studied and if possible mitigated. One of the major contributors is, as in most optical instruments, the straylight. The sources of this disturbance signal on the detector are various: e.g. the Sun, solar system bodies (moon, other planets), a mechanical part of the S/C, internal reflections inside the instrument, scattering effects. This paper will first describe the rationale behind the straylight requirement derivation based on simulated instrument performance and the design features implemented in the instrument to mitigate the straylight effects such as optical baffle, black coatings, diaphragms. In a second part, the straylight analysis performed using this design against the defined requirement will be presented. This includes both ghost images, in-field straylight and off-field straylight. The results of this analysis will finally be compared to the requirements and the design validity assessed.

Keywords: Venus, VERITAS, EnVision, VEM, EnVision, Straylight

1. INTRODUCTION

1.1 Scientific Constraints

The Venus Emissivity Mapper (VEM), also called VenSpec-M, is an infra-red push-broom spectrometer developed at DLR for both VERITAS¹ (NASA Discovery Mission) and EnVision² (ESA Cosmic Vision M6 Mission). Thanks to its very high temperature, the thermal emissions of Venus' surface occurs at relatively short wavelengths compared to what we are used to on Earth, namely around 1µm. Luckily, most of these wavelengths happen to be within the atmospheric spectral window available. It is therefore possible with VEM to map the thermal emissivity of Venus' surface from orbit, at least on Venus night side. VEM will thus exclusively operate while on the night side of Venus.³

VEM possess 14 spectral filters with different central wavelength (CWL) and bandwidth, ranging from 790nm up to 1510nm. These filters cover the atmospheric spectral windows mentioned previously but also some spectral

Further author information: martin.pertenais@dlr.de

regions used to characterize the impact of water and clouds on the spectra acquired. On top, 3 filter bands are dedicated to background measurements with a well chosen CWL placed in regions of the spectrum where no signal from Venus is expected.

From every orbit, the main scientific requirements related or impacted by Straylight are:

- Signal to Noise Ratio (SNR): for each of the 11 scientific bands (the 3 background bands have no SNR requirement, per definition) a given SNR value is required to be able to recover the emissivity accuracy needed for the mission science goals. The SNR requirements can be found in Ref. 4.
- Ground Resolved Distance (GRD): VEM is an imaging spectrometer, meaning that the spectrum has to be acquired for separate spatial parts of a scene . A spatial resolution of 100km at the surface of Venus is required.

Even though VEM operates on the night side of Venus, it is possible to have situations where the Spacecraft is actually illuminated by the Sun. This happens mostly at very high orbits. This is a major constraint for the Straylight analysis, that will be discussed in more detail in Section 3.3.

1.2 Instrument Design

The full description of the VEM instrument design is described in [5].

The main function of VEM is to acquire an image of Venus' surface in 14 separate spectral bands. The design solution implemented is to initially image Venus with a single lens on the filter assembly place on its focal plane. 14 physical spectral filters are placed on this assembly, arranged along-track so that Venus' surface (the scene) slide through the assembly one filter after the other. As shown in Figure 1, a relay optic of 2 lenses then projects the image of Venus on the filter assembly onto the focal plane assembly (FPA). The FPA is composed of an InGaAs Detector with 20µm pixels readout by an analogue chain. This design achieves a total field of view (FoV) of 45°x30°.

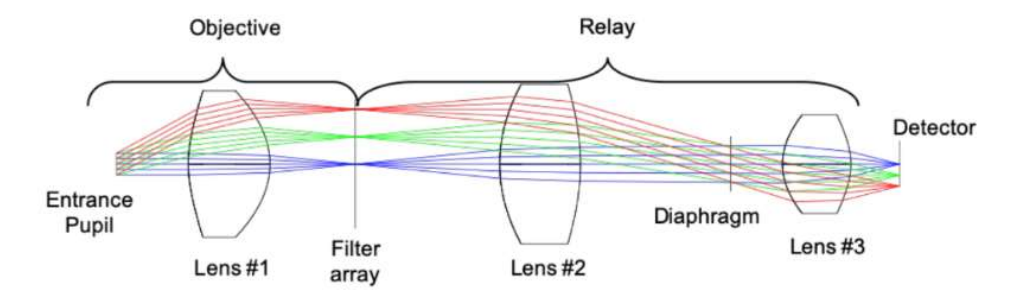


Figure 1. Optical Design of VEM.

The filter assembly is the key technological component of the instrument. The 14 filter striped (each 1.65 mm x 32mm) are glued onto a window substrate that holds a common rejection coating and a black photo-lithographic mask. Each filter substrate holds its own custom coating split onto both input and output surfaces.⁵

These 3 lenses with the filter assembly constitute the core of VEMO, the optical unit of VEM under LESIA responsibility. They are held together in a barrel-like mechanical design with an entrance pupil cone at its end and a physical diaphragm between lenses 2 and 3. In front of VEMO, a baffle cone is positioned (dark cone on the left handside of Fig. 2) to prevent straylight to enter the instrument. Because the instrument is tilted by 30° compared to the S/C panel and to allow for high temperatures due to sun illumination, a so-called Shield has to be put on top of the baffle cone. This is the most left part of the instrument on Figure 2. Its function is purely thermo-mechanical and in no-way a 'baffle' designed to reduce straylight.

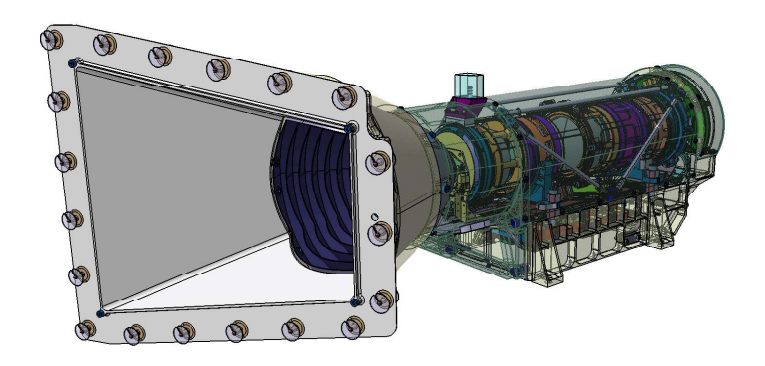


Figure 2. VEM Instrument CAD View, from Ref. 5

2. REQUIREMENT DEFINITION AND DESIGN ASSUMPTIONS

2.1 Requirement definition

In the instrument end-to-end optical performances simulator,[?] the variation of SNR for 6 filter bands has been computed as a function of the relative straylight amount. The main conclusion is that the SNR starts dropping when the number of photo-electrons coming from Straylight becomes larger than 1/10th of the number of photo-electrons coming from the Scene (Venus). This value of 10 is not a hard threshold. A value down to 5 would have a negligible impact on the SNR values.

The simulated SNR for each spectral band, without any straylight show that the weakest signal from Venus is expected for the filter 13 at 1510nm. It has a number of photo-electrons coming from the scene estimated to be 885 phe-/pixel/exposure-time. Using the factor 10 defined above, a requirement of 88.5 phe-/pixel/exposure-time can be defined. It is finally converted as per seconds to be easily used in other cases:

The Straylight signal on the detector shall not exceed 960 photo-electrons/pixel/s.

Note: this includes out-of-field straylight (from the Sun or S/C parts in the FoR), in-field straylight due to contamination, ...etc

In order to verify this requirement in a more easy way in the analysis (especially for the in-field straylight), it can be converted into an irradiance ratio between the scene and the acceptable straylight. In-field, the only possible source of straylight is actually Venus scene, with bright points on the surface (or atmosphere) cross-contaminating other positions on the detector. With that in mind, we can consider the highest possible irradiance ratio expected from Venus. From the simulations, this ratio is in the order of magnitude of 5%, with 41 000 photons/pixel/exposure for the brightest band at 1180nm and 2200 photons/pixel/exposure for the weakest band at 1510nm. The factor of 10 mentioned above needs then to be applied on top of this value to ensure that the straylight from the strongest band has no impact on the SNR of the weakest band.

Instead of requiring the straylight to be less than 960 e-/pix/s as done above, it is equivalent to require the in-field straylight (ghost images) to be less than 0.5% in terms of irradiance between the source signal and its created straylight on the detector.

2.2 Design Assumptions for the Analysis

As input for the Straylight analysis, each opto-mechanical surface of the instrument need to be described by some key parameters: the reflectance, the transmittance, the roughness, the contamination levels. Table 1 shows an overview of these parameters for the all the relevant surfaces.

The reflectance value reported in the table is an average value across the spectral range. For the simulation in LightTools software, full spectral responses were used. Where possible, Bi-Directional Scattering Distribution Functions (BSDF) were measured on samples and used as input for the simulation.

Surface	Coating	Reflectance	Roughness	Contamination
1st Lens	None	Fresnel coef.	5nm RMS	1425ppm
Lenses	None	Fresnel coef.	5nm RMS	500ppm
Mechanics around lenses	KeplaCoat or Surtec	Figs. 3,4	_	500ppm
Entrance Pupil + Diaphragm	MAP AQPU1 ⁶	5%	_	500ppm
Baffle Shield	Ceranovis ACF V14 ⁷	80%, Fig. 5	_	5000ppm
Baffle Cone	KeplaCoat or Surtec	Figs. 3,4	_	5000ppm
Spectral Filters	CILAS narrow band	100% out of range	_	_
Mechanics around Filters	CILAS black	5%	_	500ppm
Sensor	NA	25% (1-QE)	_	_
Mechanics around sensor	Gold	98%	_	500ppm
Sensor Sapphire Window	AR coating	4%	5nm RMS	500ppm
FPA Baffle	. Baffle KeplaCoat		_	500ppm

Table 1. Surface parameters overview.

For most of the mechanical surfaces, an open point to be clarified thanks to the straylight analysis was the need to use a black coating (KeplaCoat) or not (usual Surtec treatement). Both samples were analysed and measured. The BSDF of the KeplaCoat on Aluminium 7075 is plotted for two wavelengths in Fig. 3. The Total Integrated Scatter (TIS) was measured to be 5% at 850nm and 20% at 1550nm. The BSDF of the Surtec on Aluminium 7075 is plotted for two wavelengths in Fig. 4. Its TIS was measured to be 45% at 850nm and 80% at 1550nm.

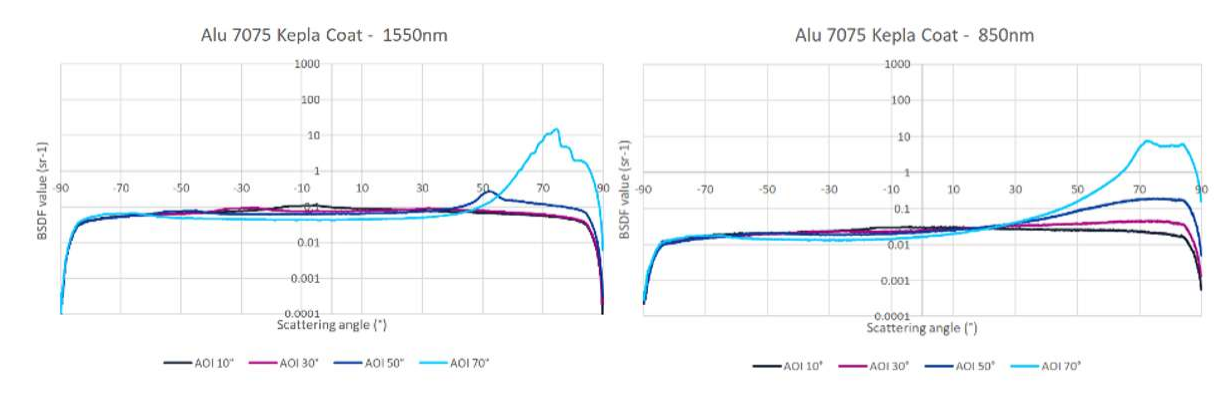


Figure 3. Measured BSDF of black KeplaCoat on Al 7075.

Similarly, the BRDF of a white Ceranovis V14⁷ sample was measured at DLR. As shown in Fig. 5, the reflectance response of the this white paint is very close to be a perfect Lambertian function. Indeed, the measured reflectance is almost independent from the incidence angle of the light (the 3 different curves in the plot) and follows the natural cosinus function of the equivalent surface view factor. Its TIS was also measured and is, as expected, very high with values ranging from 88% at 800nm and 73% at 1600nm.

Finally, the real designed spectral responses (transmission and reflection curves) of each individual filter band was used in the simulation. They provide a very high transmittance (90%) within their narrow band specified and a very high reflectance (> 99%) out of this range, meaning for most of the spectral range. In terms of straylight, these filters bands will therefore be one of the worst contributors, being basically mirrors on an intermediate focal image plane.

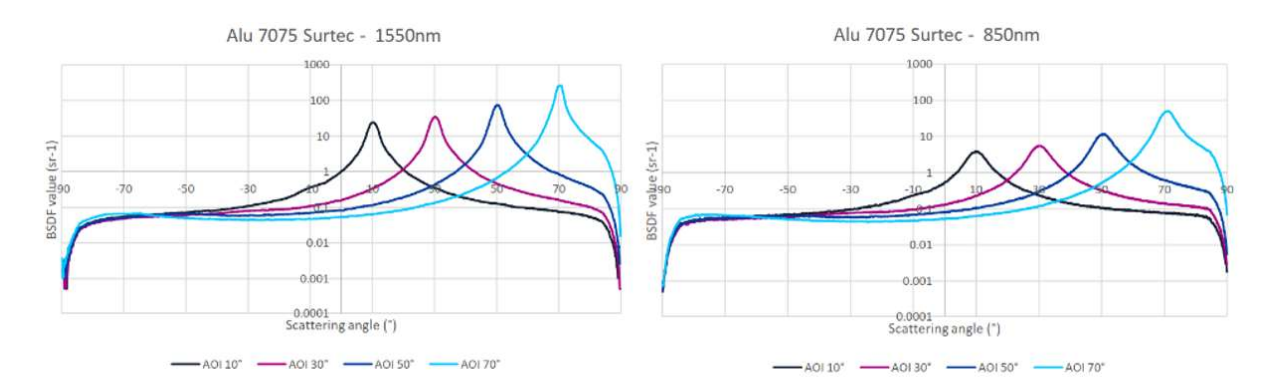


Figure 4. Measured BSDF of black KeplaCoat on Al 7075.

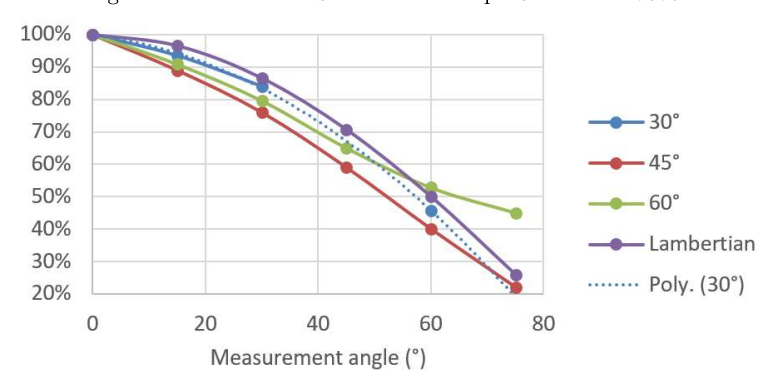


Figure 5. Measured BRDF of a white Ceranovis V14 sample.

3. STRAYLIGHT ANALYSIS AND RESULTS

The simulation was performed with the LightTools software, using the inputs described in the previous section and the most recent CAD Model of the whole instrument.

The analysis was performed in three steps:

- 1. in-field straylight analysis with only the optical elements in the model (ghost analysis).
- 2. addition of the mechanical surfaces around the optics. Main goal of this part is to check the impact of the mechanical surfaces, identify the worst contributor and establish the need for a black coating.
- 3. Off-field straylight analysis with the baffle in front of the instrument. The goal of this part is to verify the efficiency of our baffle assembly, and especially decorrelate the efficiency of its geometry from its coatings.

The analysis was performed with black KeplaCoat⁸ on the mechanical surfaces, and then repeated with classical Surtec reflective treatment. No measurable difference in the straylight levels on the detector was detected between these two cases. This confirms the fact that no black coating is necessary on the internal surfaces of the instrument. Note that this is valid and simulated only for source within the optical FoV of VEMO. This conclusion is therefore applicable only in the presence of the Baffle Assembly blocking any out of field direct straylight into VEMO.

Similarly, the simulation was performed with and without contamination, and with and without surface roughness values on the lenses. Again, no relevant increase of the Straylight level was detected between all of these cases, confirming the current cleanliness budget and roughness values of the lenses.

	Table 2. Relevant nignest irradiance gnosts on-axis.								
	1st element	surface	2nd element	surface	Relative Irradiance				
1	Sapphire	2nd	Filter#6	1st	0.0029%				
2	Sapphire	1st	Filter#6	1st	0.0023%				
3	Sensor	-	Sapphire	2nd	0.0021%				
4	Sapphire	2nd	Filter#8	2nd	0.0019%				
5	Sapphire	1st	Filter#8	2nd	0.0015%				
6	Sensor	_	Sapphire	1st	0.0014%				
7	Lens#2	2nd	Filter#9	2nd	0.0010%				
8	Filter#7	1st	Lens#1	1st	0.0010%				
9	Lens#2	2nd	Filter#10	2nd	0.0010%				
10	Filter#7	1st	Lens#1	1st	0.0008%				
11	Lens#2	2nd	Filter#6	1st	0.0008%				
12	Lens#3	2nd	Lens#3	1st	0.0007%				
13	Lens#2	2nd	Filter#8	2nd	0.0007%				
14	Sensor	_	Lens#2	2nd	0.0003%				
15	Sensor	_	Lens#2	1st	0.0001%				
16	Sensor	_	Lens#3	2nd	0.0001%				
17	Sensor	-	Lens#3	1st	0.0001%				

Table 2 Relevant highest irradiance ghosts on-axis

3.1 Ghost Images Analysis

For this part of the simulation, the straylight source was chosen to be a perfect point source, placed at several positions within the optical field of view of the instrument: on-axis, at the field edge along X and at the field edge along Y.

An example of the output image simulated on the detector in shown on Fig. 6. Several individual ghost images are created by multiple reflections inside the instrument. The most powerful ghosts are actually falling back on top of the nominal image and were therefore not considered in the analysis and requirement verification. They come mostly from back-reflections between the sensor assembly (either sensor itself or the window in front of it) and the filter stripe on which the point source was focused.

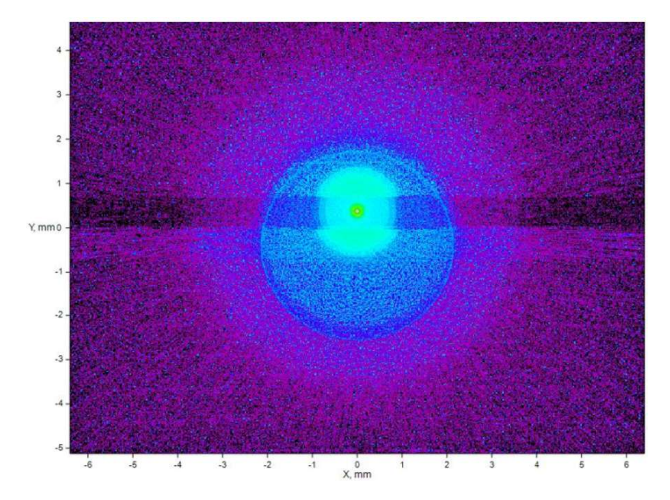


Figure 6. Example of Straylight Image for a point-like source placed closed to the optical axis

The relative irradiance for all the remaining relevant ghosts was computed in order to compare it to the requirement of 0.5% relative irradiance derived in Section 2. Table 2 presents the list of ghosts for the on-axis case.

Considering the requirement of 0.5% as a limit, the margin is very high even if we consider as an unrealistic worst case that all these ghosts fall on top of each other, with a sum of these 17 ghosts of 0.019%. The same analysis was performed for a point source placed at the maximum vertical (along-track) and horizontal (across-track) field of view and provided comparable results.

3.2 Extended Source Analysis

The previous chapter has shown that for a point-like source, the straylight level created remains well within the acceptable science requirement. However, during science operation this case will not be realistic as VEM will constantly observe Venus' surface and be fully illuminated. To cover this case, an extended source was simulated in the software to cover the complete FoV of VEM and fully illuminate the detector. This source cover exactly VEM FoV and has a flat spectrum from 750 to 1550nm.

Figure 7 below show the output of the simulation, with the complete image split in two: on the left side the image detected on the detector with only the rays coming straight from the source (the signal) and on the right hand side the image on the detector with only the straylight rays, reaching the detector after at least one non-nominally reflection in the instrument. The sum of both images per pixel would provide the 'real' image considering all the rays. Note the factor of 10 difference in the color scale between both images.

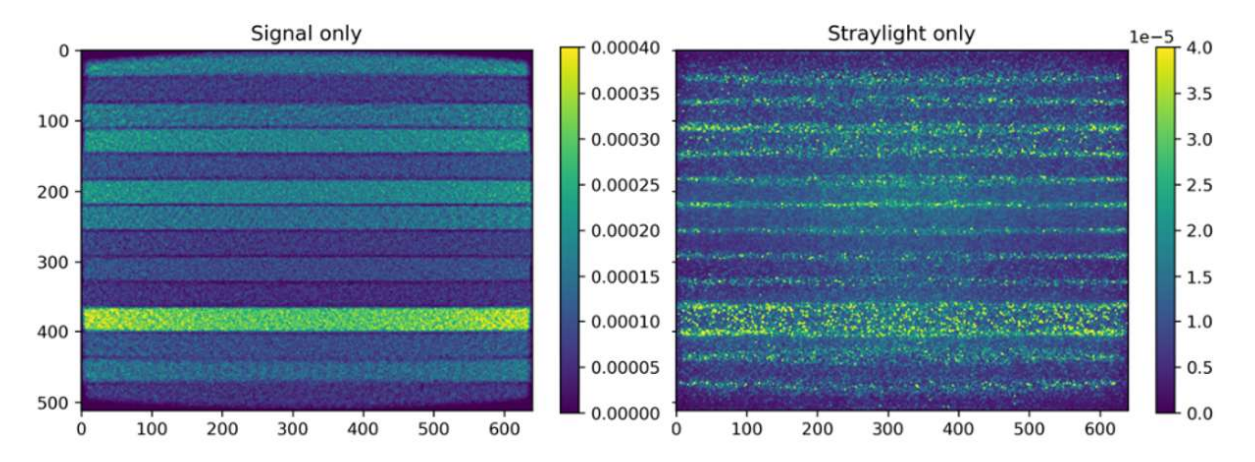


Figure 7. Left: image detected with a flat field illumination considering only direct rays. Right: same image with only Straylight rays considered

While we could have expected an homogeneous intensity on all the detector on the left hand side image of Fig. 7 with a flat spectrum as input, the observed intensity level difference between filter directly correlate with the spectral width of their spectral response. Indeed, the wider the spectral response, the more photons make it through that filter and are detected on the image. For example filter 11 (around line 380), with the wider spectral response (60nm FWHM) shows clearly a much higher detected intensity that the other filters. The integrated flux from the Straylight on the detector is a factor 11 lower than the total integrated flux from the image, which is smaller than the requirement of having at least 10 times less straylight than signal. Considering that for each point-source, at least 20% of the straylight flux actually focuses on the nominal image and is therefore not counted as Straylight but as useful signal. On top of that, another 10% of the straylight flux is caused by internal reflection inside the detector between the sensitive surface and the protective Sapphire window in front of it. These ghosts are not considered as focused on top of the image but produce a halo around the image. As this energy is also remaining inside a filter band and not contaminating the neighboring ones, it can be removed from the analysis. By removing these 31% of the straylight flux, the ratio between the Signal and Straylight levels per detector line is plotted in Fig. 8

The factor of 10 requirement is met on all the filter band except marginally for filter band 10 (around line 350). The background level of Straylight causing this marginal non-compliance is impacting the bands with lower signal. The fact that filter band 10 is impacted in this simulation is purely due to the fact it has the narrower

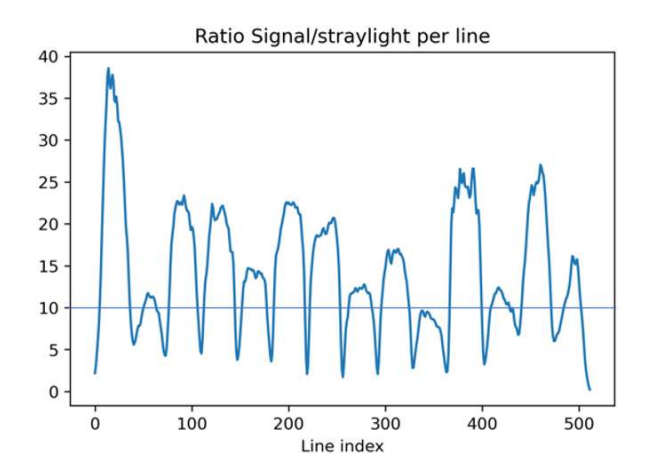


Figure 8. Integrated signal/straylight ratio per detector line, compared to the requirement of 10.

spectral response and therefore the lowest integrated signal in this simulation. The real conclusion here is that we can expect a straylight level for bands with low signal of down to 8 times the signal level.

This is not expected to put the scientific SNR requirement at risk because of several reasons. The value of 10 was a very conservative choice of requirement for which no SNR degradation is measurable. Using a value 8 instead, provides a SNR degradation of less than 2% and is therefore fully compatible with the available margins at system level. On top of that, this simulation case with a full flat field illumination is obviously a very unrealistic worst case. In practise, we expect a scene of Venus with a mixture of bright and dark regions for each of the filter bands, bringing the integrated straylight level down.

3.3 Off-Axis Analysis

The Point-Source-Transmittance (PST) is a classical way of characterizing the straylight response from an optical instrument. It is defined as the average irradiance on the detector Irr_d and the irradiance of the straylight source Irr_s at the entrance of the instrument. It can be understood as an angle dependent rejection factor of the instrument.

$$PST = \frac{Irr_d}{Irr_s},\tag{1}$$

With the irradiance being the ratio of the flux (in watts, or photons/s for example) and the area of the surface, the PST Definition becomes:

$$PST = \frac{Flux_d}{Flux_s} \cdot \frac{Area_s}{Area_d} \,, \tag{2}$$

The source was positioned at the entrance of the baffle shield as shown on Fig. 9 below. It created a constant and homogeneous collimated beam of 1W. The directional vector of the collimated beam could be varied along both X (called azimuth in the simulation, across-track for the missions) and Y (called elevation in the simulation, along-track for the mission) axis.

With $Flux_s = 1W$, $Area_d$ (1.31 cm²) and $Area_s$ (384 cm²) being constant physical sizes in the instrument, the only unknown to compute the PST is the flux received by the detector. The off-field simulation consisted therefore in measuring the detected flux on the detector as a function of both azimuth and elevation angles at the entrance of the instrument.

Because of the strong spectral dependence of the instrument and to create a realistic simulation, it was decided to use the solar spectrum as source spectrum. To make sure that only the photons falling in the detectable spectral range of the detector, the solar spectral irradiance was combined to the quantum efficiency curve of the detector.

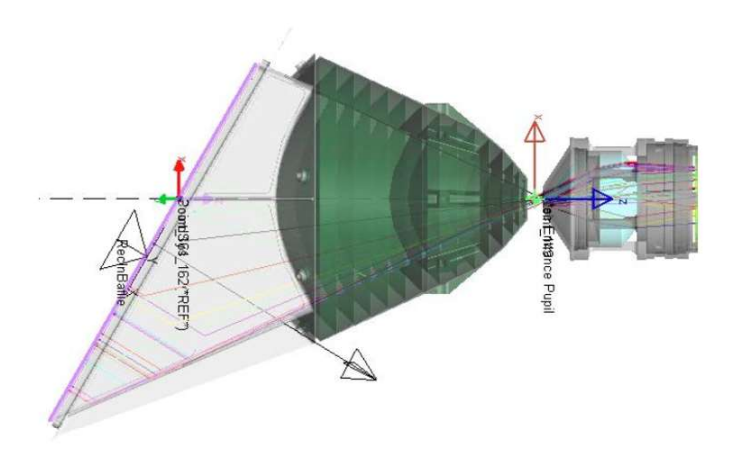


Figure 9. Top view of the instrument entrance for the off-field simulation. The pink 'cap' closing the baffle shield opening is the 1W source used for the PST computation.

The main source of straylight for the off-field study is the Sun. Indeed, even if we operate our instrument on the Venus night side, it can happen (especially at high altitudes orbit) that the spacecraft is illuminated by the Sun. In practice this means that we will have the sun positioned very close to the edge of our field of view. To map all the possibilities, it was decided to run the simulations with the Sun (represented by the collimated light source at the baffle shield opening) anywhere in the hemisphere in front of the instrument:

- +/-90° around the optical axis in elevation (Y-axis of the instrument, along-track, short side of the detector)
- -60°/+120° around the optical axis in azimuth (X-axis of the instrument, across-track, long side of the detector

The asymmetry on the azimuth direction comes from the fact that the instrument opening is tilted by 30° compared to the optical axis normal plane.

Figure 10 shows the output of the analysis, with the PST for 8 different azimuths angles, across the full \pm 0° elevation range.

The first observation is that for every single azimuth computed, the PST appears to be symmetrical across the $+/-90^{\circ}$ elevation space. This is logical considering that the whole instrument is symmetrical along that axis, especially the baffle shield. To the contrary, it is visible that the PST with azimuth values in the positive side ($+30^{\circ}$ and $+45^{\circ}$) are up to an order of magnitude higher than the ones on the negative side (-30° , -45° and -55°). Again, this asymmetry was expected considering the geometry of the baffle shield. With azimuths values higher than 0° , the longer part of the baffle shield, which is highly reflective, is illuminated by the source. This is causing more straylight rays to enter the instrument than on the other side, where the baffle shield length is minimal. This shows that the Ceranovis V14ACF white paint⁷ on the Baffle Shield is the driving parameter of this simulation. This is confirmed by the looking in details at the ray tracing and which reflections are the bigger contributors to the PST.

The first reflection for off-field straylight rays always occurs on the baffle shield. This means indirectly that all the rays hitting the baffle cone (in green in Fig. 9) are trapped and do not manage to reach the detector. The important question to answer is if this is thanks to the cone geometry or thanks to its black coating, or both. The PST computation was repeated with a reflective Surtec coating on the baffle cone substrate instead of the black Kepla-Coat. Figure 11 shows the comparison for 2 different azimuths (all others lead to the exact same conclusion but bring confusion in the plot) of the PST with black Kepla-Coat and with reflective Surtec. There is no significant difference or trend between the curve to conclude on any impact of the coating on the PST. The differences are considered to be in the simulation noise/uncertainties. This would induce that the rejection function of the baffle cone is exclusively performed by the intrinsic geometry of the cone and not by its coating.

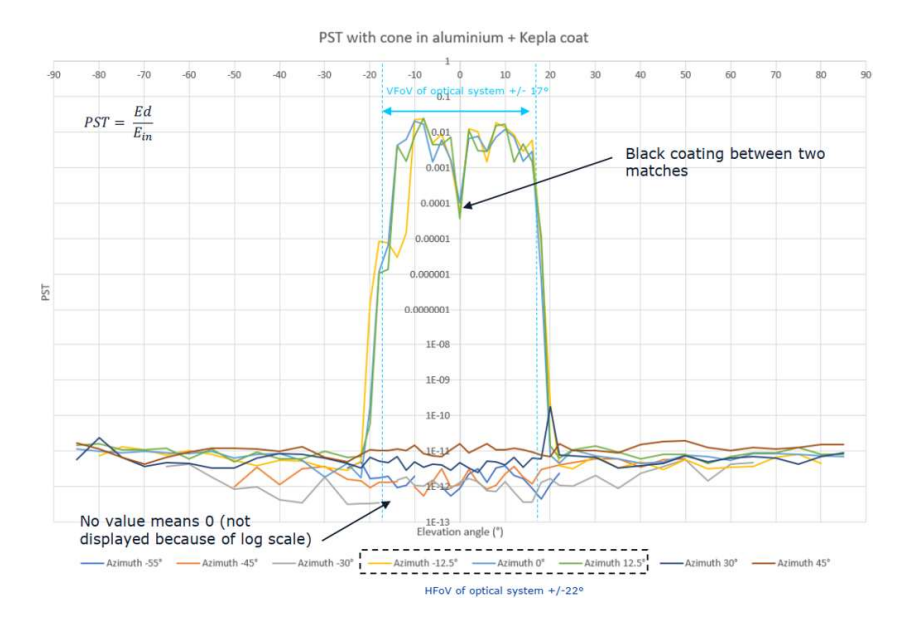


Figure 10. Results of the off-field analysis. The PST computed is between 10^{-11} and 10^{-12} for every azimuth and elevation outside of the instrument field of view

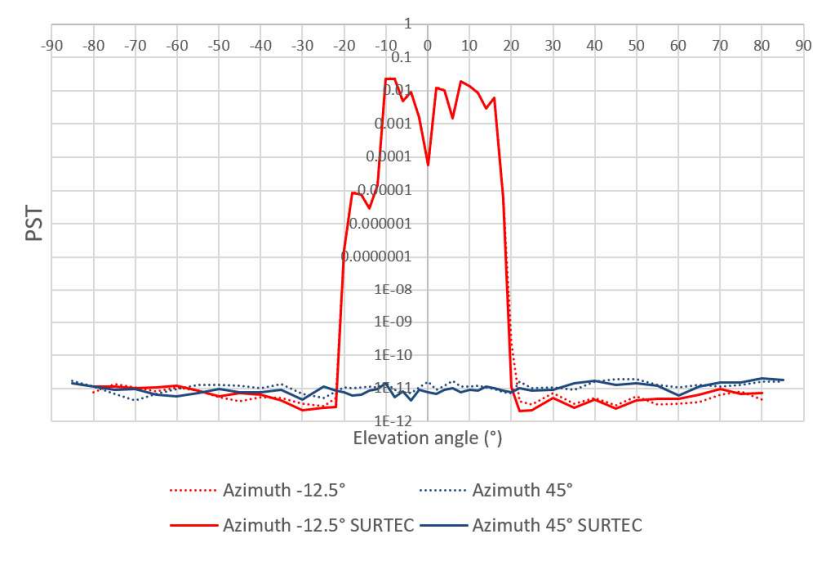


Figure 11. PST Comparison between KeplaCoat (dashed lines) and reflective Surtec (full lines) coatings on the baffle cone

To close the analysis from these computed PST to the scientific requirements, a 2D PST map was created to be able to compute the final straylight level for every single sun position in the hemisphere in front of the instrument. While for the $+/.90^{\circ}$ elevation axis enough sampling was available to apply a standard interpolation function, the small discrete number of azimuth curves was not sufficient. Azimuthal regions were therefore defined in which a constant PST value was taken, using the 8 available elevation curves showed in Fig. 10.

Figure 12 shows the result of this exercise shown in log scale (left). This 2D map needs to be understood that way: the color value at one point of the map (full hemisphere in front of the instrument) provides the PST (irradiance rejection factor) for a source (e.g. the sun) placed at that position in front of the instrument.

The same conclusions based on the individual PSTs are also visible:

- The positive side of the along-track axis (azimuth) has a significantly higher PST than the negative side, due to the baffle shield geometry
- The PST is symmetrical on the across-track direction
- The PST value oscillates between $< 10^{-12}$ and 5.10^{-10} outside of the field of view

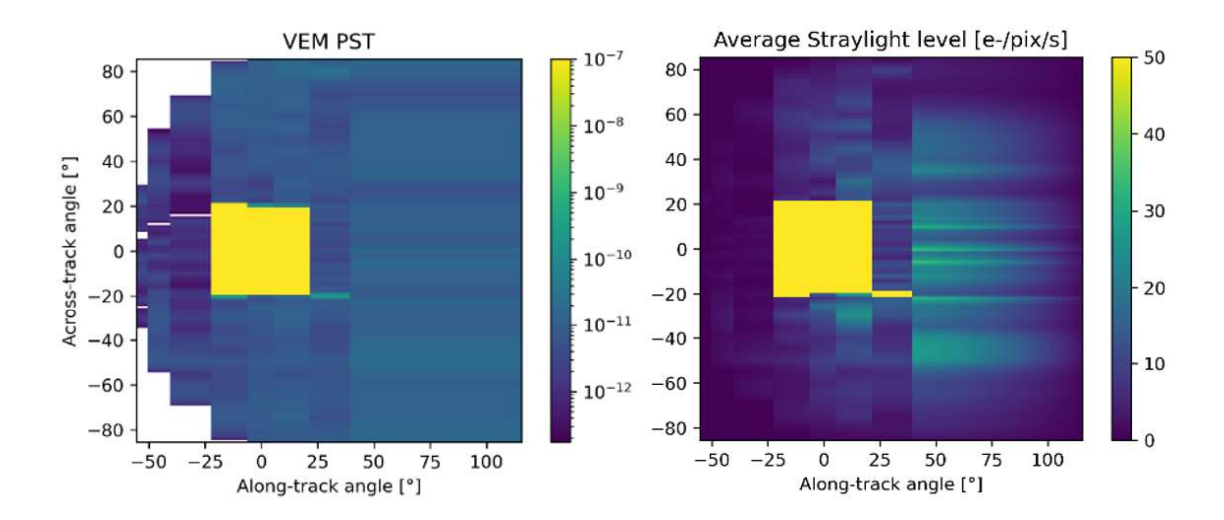


Figure 12. Integrated signal/straylight ratio per detector line, compared to the requirement of 10.

In order to convert this PST into a number of photo-electrons per pixels per second to compare to the requirement, it first needs to be corrected by the viewing factor of the opening of the baffle. Indeed, the PST was computed with a fixed source placed inside the opening. In reality, a factor $\cos(\text{elevation})^*\cos(\text{azimuth})$ needs to added to the PST. For every point of the hemisphere in front of the instrument, this corrected PST can be multiplied to the actual input spectral irradiance of the sun, rescaled to the quantum efficiency. This provides then the detected irradiance by the detector (in $W/m^2/nm$):

$$Irr_{detected}(\lambda, az, ele) = Irr_{sun@venus}(\lambda).QE(\lambda).PST(az, ele).\cos(az).\cos(ele), \qquad (3)$$

For every wavelength, this irradiance can then be converted into a spectral photo-electron irradiance using the Planck constant and the celerity of light to obtain a detected spectral energy in photoelectrons/s/ m^2 /nm. Knowing the size of a pixel in m^2 and integrating the spectrum into a total value, the final number of electrons/pixel/s can be computed for every position of the sun in front of the instrument.

$$Straylight(az, ele) = \int_{500}^{2000} Irr_{detected}(\lambda, az, ele) \cdot \frac{\lambda}{h.c} \cdot Area_{pixel} \, d\lambda , \qquad (4)$$

The resulting map from this equation is shown on the righ-hand side of Fig. 12.

On the lower right corner of the detector, there seems to be bright spot/stripe, not fully compatible (by eye) to the rest of the values. This point is real, and can be traced back to the peak of the PST in at the elevation 20° and azimuth 30° . Looking in details at the raytracing, this relatively high PST comes from one single ray that reaches the detector after 5 reflections. By deleting this one single ray manually, the PST at this point drops by a factor of 3, from 2.10^{-10} to 6.10^{-11} , or from 370 to 120 e-/pix/s. Note that in any case, both values are

still compliant. But this shows the limit of such simulations, with results based on a very little number of rays considering the very high rejection factor of this instrument.

Except for this one single point, the average straylight level remains lower than 40 e-/pix/s. This needs to be compared to the requirement derived in Section. 2 of 960 e-/pix/s.

The conclusion of this off-field analysis, is that even in the absolute worst case of having the Sun right at the edge of our field of view during science operation of Venus night side, the straylight level induced are not even detectable and therefore do not impact the SNR requirements.

4. CONCLUSIONS

The simulations presented in this paper showed the full end-to-end Straylight analysis for the VEM instrument. It has been proven that per design, the instrument is very insensitive to bright object out of its field o view. With a rejection factor of 10^{-11} outside of the FoV, even placing the Sun at the very edge of the optical FoV doesn't create any detectable straylight on the detector. A value of 40 e-/pixel/s was computed, to be compared with the requirement of 960 e-/pixels/s. This is valid for a design baseline where no black coating is applied on the baffle cone in front of the instrument.

As for the in-field analysis, it has been shown that the surface treatment of the mechanics inside the optics barrel plays no role in the straylight, assuming the baffle assembly is blocking the direct out of field light paths. The same applies for the contamination level and the micro-roughness of the lenses surfaces. On the other hand, some key mechanical surfaces have a direct impact on straylight and should be kept with the baselined black coating: the inside of the entrance pupil, the area around the filter stripes, the diaphragm between lenses 2 and 3 and the FPA Baffle in front of the detector.

Individual ghosts are well within the requirement by a factor of at least 5 by combining them. Without summing them all up, the worst ghost has a relative irradiance of 0.027% compared to the nominal image. This has to be compared to the requirement of 0.5%. By considering an extended source illuminating the complete detector, which is the absolute worst case, a marginal non-compliance was found with some areas on the detector showcasing a factor of 8 between the signal and the straylight level. A factor of at least 10 was required. This background level of Straylight is mostly driven by:

- The reflectance of the sensor (Sapphire Window, sensitive area and golden lid around it)
- The reflectance of the filter stripes
- The reflectance of the lenses surfaces

This marginal non-compliance is not considered as critical as it appeared during a worst case computation and because this factor of 10 could be challenged. However, the recommendation would be to reduce as much as possible the reflectance values listed above. We understand this is not possible for the sapphire window (as part of the detector package), the sensitive area (linked to the quantum efficiency), the filter stripes. In the simulations, no anti-reflection coatings were considered on the lenses, this would be first and easiest measure to implement. The second one would be to design a less reflective surface (or surface treatment) in front of the golden lid around the detector.

Summary of design impacts:

- No need for black coating inside the baffle cone
- No need for black coating inside the optics barrel
- Need for black coating in the critical optics areas (around the filters, inside the entrance pupil and on the diaphragm)
- Need for AR coating on lenses
- Need for black coating on FPA baffle
- Need to hide the gold lid from detector, or make it less reflective

REFERENCES

- [1] S. E. Smrekar, e. a., "VERITAS (Venus Emissivity, Radio Science, InSAR, Topography, and Spectroscopy): A Discovery Mission," in [2022 IEEE Aerospace Conference (AERO)], 1–20 (2022).
- [2] A. G. Straume-Lindner, e. a., "Science objective and status of the EnVision mission to Venus," *Proc. SPIE* **18247** (2024).
- [3] J. Helbert, e. a., "The Venus Emissivity Mapper (VEM): obtaining global mineralogy of Venus from orbit," in [Infrared Remote Sensing and Instrumentation XXVI], Proc. SPIE 10765 (2018).
- [4] J. Helbert, e. a., "The Venus Emissivity Mapper (VEM): advanced development status and performance evaluation," in [Infrared Remote Sensing and Instrumentation XXVIII], Proc. SPIE 11502 (2020).
- [5] T. Hagelschuer, e. a., "The Venus Emissivity Mapper (VEM): Instrument design and development for VER-ITAS and EnVision," in [Infrared Remote Sensing and Instrumentation XXXII], Proc. SPIE 13144 (2024).
- [6] AQPU1. https://www.spacematdb.com/spacemat/manudatasheets/MAP-PU1%20DS.pdf. (Accessed: August 2024).
- [7] Hołyńska, M., Butenko, Y., Martins, R., Semprimoschnig, C., Meyer, F., and Faber, S., "Studies of White Ceramic Coatings for ESA's BepiColombo Mission to Mercury," *Journal of Spacecraft and Rockets* **56**, 1–13 (05 2019).
- [8] Aalberts. https://www.aalberts-st.com/processes/plasma-chemical-coatings/. (Accessed: August 2024).